Interpreting Diffusion Models in Koopman Space via CLIP Alignment

Aurelien Ghiglino [1] **Anirban Roy** [2] **Colin Samplawski** [2] **Ramneet Kaur** [2]

Abstract

We present a method for interpreting diffusion models by aligning the latent space of a Koopman-distilled generator with CLIP's semantic embedding space. A lightweight encoder-decoder is trained on top of a frozen Koopman Distilled Model to produce a bidirectional mapping that enables black-box semantic steering. We introduce an inference-time constrained optimization procedure that disentangles concepts by protecting non-target attributes while moving along a desired concept direction. Experiments show that this approach reduces non-target drift and improves semantic stability compared to the naive baselines, enabling more disentangled and interpretable image manipulation.

1. Introduction

Diffusion models are difficult to interpret due to their complex denoising process. Koopman Distilled Models (KDM) offer a promising alternative by lifting diffusion trajectories into a linear latent space, making semantic structure more accessible (Berman et al., 2026). Thus we propose a framework that aligns KDM latents with CLIP embeddings, enabling semantic editing without modifying the underlying generator. Our contributions are:

- **Black-Box Interpretability**: all edits occur in Koopman space with the diffusion model frozen.
- **No Curated Concept Dataset for Finding Directions**: CLIP text embeddings define semantic axes.
- **Inference-Time Disentangling**: novel inference time optimization objective preserves non-target attributes.
- **Adaptive Steering Strength**: adaptively selected uniform semantic steps instead of static steering.

This alignment turns Koopman latents into a semantically navigable space, enabling disentangled edits driven by CLIP while treating the underlying generator entirely as a black box.

2. Related work

Diffusion Model Latent Spaces Prior work has explored diffusion latents through Riemannian geometry (Park et al., 2023), CLIP-based (Radford et al., 2021) guidance in latent space (Becker et al., 2025), and semantic directions in U-Net bottleneck features Sparse Autoencoder (SAEs)(Tinaz et al., 2026). Self-Guidance (Epstein et al., 2023) shows that activations within diffusion U-Nets encode object-level properties such as position, shape, and appearance. Attention-based editing methods such as Prompt-to-Prompt (Hertz et al., 2022) demonstrate that cross-attention maps within diffusion U-Nets encode the spatial relationship between pixels and text tokens, enabling image edits through prompt manipulation alone. Our work instead performs semantic interpretation and control on top of a fully trained diffusion model treated strictly as a black box.

Koopman Operators in Diffusion Koopman (1931) operators provide a linear representation of nonlinear dynamics by lifting the system into a higher-dimensional space where its evolution becomes a single linear transformation. Most relevant to our work, Hierarchical Koopman Diffusion (HKD) (Bai et al., 2026) lifts diffusion dynamics into a globally linear latent space, and Koopman Distilled Models (KDM) (Berman et al., 2026) perform one-step diffusion by encoding models into Koopman representations that preserve semantic structure. We extend KDM by aligning its latent space with CLIP for interpretability.

3. Methodology

Koopman Distillation Model (KDM) Let us summarise the KDM framework of Berman et al. (2026). A pre-trained diffusion model defines a deterministic mapping $\Phi_T : \mathbb{R}^n \to \mathbb{R}^n$ from Gaussian noise $x_T \sim \mathcal{N}(0, \sigma_T^2 I)$ to clean data $x_0 = \Phi_T(x_T)$. KDM models this mapping as a single-step linear evolution in a learned embedding space:

$$x_0 \approx D_\psi(C_\eta E_\phi(x_T)),$$

[1]Aerospace Design Laboratory, Stanford University, USA [2]Computer Science Laboratory, SRI International, USA. Correspondence to: Aurelien Ghiglino <aghig@stanford.edu>, Ramneet Kaur <ramneet.kaur@sri.com>.

Preprint. August 4, 2026.

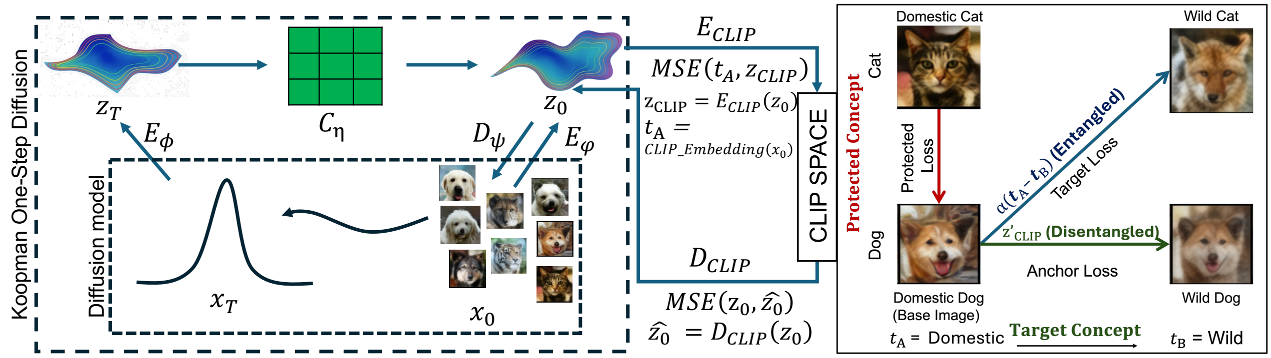

Figure 1. Overview of the KDM-CLIP alignment architecture. A frozen KDM maps diffusion noise to Koopman latents, which are then projected into CLIP space via a trainable encoder E_{CLIP} and mapped back via D_{CLIP}. CLIP image embeddings provide fixed semantic targets, enabling interpretable alignment between Koopman dynamics and CLIP's semantic space.

where $E_\phi : \mathbb{R}^n \to \mathbb{R}^d$ is a noise encoder, $C_\eta \in \mathbb{R}^{d\times d}$ is the learned Koopman operator (a linear layer), and $D_\psi : \mathbb{R}^d \to \mathbb{R}^n$ is a decoder. A complementary image encoder E_φ encodes clean images into the same latent space. The training objective combines reconstruction, latent consistency, prediction, and adversarial losses. Henceforth, we denote the Koopman-evolved latent as $z_0 = C_\eta E_\phi(x_T)$.

KDM-CLIP Our goal is to learn a mapping between the Koopman latent space and the CLIP embedding space that is (a) semantically faithful, (b) invertible, and (c) allows the generative model to be treated as a black box. We achieve this by training an encoder-decoder from Koopman space to CLIP space, denoted by E_{CLIP} and D_{CLIP}, on top of a fully frozen KDM. The complete pipeline is illustrated in Fig. 1. Starting from the KDM-produced latent z_0 of a generated image x_0, the model learns a CLIP-space alignment by (1) extracting a CLIP embedding t_A of the target image x_0, (2) predicting a matching CLIP embedding z_{CLIP} via a trainable adapter $E_{\text{CLIP}}(z_0)$, and (3) decoding z_{CLIP} back into the Koopman latent space with $\hat{z_0} = D_{\text{CLIP}}(z_{CLIP})$. The total training loss is

$$\begin{aligned}\mathcal{L} &= \mathcal{L}_{\text{enc}} + \lambda_{\text{dec}}\mathcal{L}_{\text{dec}} \\ &= \text{MSE}(t_A, z_{CLIP}) + \lambda_{\text{dec}}\text{MSE}(z_0, \hat{z_0}), \end{aligned} \quad (1)$$

where MSE is the Mean Square Error and λ_{dec} balances the two objectives. All KDM parameters (E_ϕ, C_η, D_ψ) and the CLIP model for t_A remain frozen throughout training.

Semantic Steering via CLIP Text Directions Given the trained E_{CLIP} and D_{CLIP}, we perform inference-time semantic editing. Steering directions in this work are derived from contrastive concept pairs (A, B) (e.g., "young animal" vs. "old animal"). Each concept in the pair is defined by the user as set of n prompts ($n = 8$ in our experiments: examples are in Appendix A.2). We embed each prompt with the CLIP encoder, and the normalized averages of these prompts are used to obtain the target embeddings t_A, and t_B.

Given the Koopman latent z_0 for a base generated image x_0, we first map it to CLIP space $z_{\text{CLIP}} = E_{\text{CLIP}}(z_0)$, steer the embedding z_{CLIP} to obtain z'_{CLIP}, decode z'_{CLIP} back to the Koopman space and synthesize via the frozen KDM decoder $x'_0 = D_\psi(D_{\text{CLIP}}(z'_{\text{CLIP}}))$.

A naive additive delta $z'_{\text{CLIP}} = \text{normalize}(z_{\text{CLIP}} + \alpha(t_A - t_B))$, where α is the steering strength, often causes unintended changes to attributes unrelated to the target concept t_A. We, therefore, adopt a constrained steering approach. For a base image x_0, we detect which concepts are strongly present by scoring z_{CLIP} against a curated vocabulary of CLIP embeddings corresponding to a set of prompts representing the data distribution. There can be different ways of generating the curated set of prompts representing the data and details on the process followed in the paper are in Appendix A.1. At inference, prompts (from the curated set) whose text overlaps with the target concept are excluded, and the remaining set $\{t_i\}$ of prompts representing different concepts are chosen based on highest ranking via $\cos(\text{CLIP}_{\text{img}}(x_0), \text{CLIP}_{\text{txt}}(t_i))$. $\{t_i\}$ forms the protected set $\mathcal{P}$.

We then optimize the new latent z'_{CLIP}, by minimizing the loss $\mathcal{L}_{\text{steer}}$

$$\begin{aligned}&= -\lambda_t \underbrace{\left[\alpha\ (\cos(z'_{\text{CLIP}}, t_A - t_B) - \cos(z_{\text{CLIP}}, t_A - t_B))\right]}_{\text{target gain}} \\ &+ \lambda_p \underbrace{\frac{1}{|\mathcal{P}|}\sum_{i\in\mathcal{P}} \left(\cos(z'_{\text{CLIP}}, t_i) - \cos(z_{\text{CLIP}}, t_i)\right)^2}_{\text{protected concept drift}} \\ &+ \lambda_a \underbrace{\left(1 - \cos(z'_{\text{CLIP}}, z_{\text{CLIP}})\right)}_{\text{anchor}} \end{aligned} \quad (2)$$

The target term drives the edit in the desired direction, the protection term penalizes drift in CLIP similarity for concepts in the image disjoint from the target, and the anchor term is a regularizer that prevents the latent from drifting too far from the original image in the CLIP embedding space. λ_t, λ_a, and λ_a define the weightage to each term respectively. α is dynamically selected based on the desired steering strength, defined by

$$\cos\left(\frac{z_{\text{CLIP}} + \alpha d}{\|z_{\text{CLIP}} + \alpha d\|}, z\right), \tag{3}$$

where $d = \frac{t_A - t_B}{\|t_A - t_B\|}$ is the normalised contrastive CLIP text direction. This is different from the existing work on steering with fixed α determined from a validation set for each concept (Zou et al., 2023; Beaglehole et al., 2026). After optimizing z'_{CLIP}, it is normalized to form the final steering direction.

4. Experimental Results

We perform our experiments on Animal Faces-HQ (AFHQ) Dataset (Huang et al., 2025). This dataset of high-quality images at 512×512 resolution. There are three domains of classes: cat, dog, and wildlife, with diverse images of various breeds per each domain in the dataset. This is one of the HQ datasets used by Berman et al. (2026), enabling us to use their trained KDM model.

Evaluation Metrics: We evaluate each steered image x'_0 against its original x_0 using the following three metrics:

1. Target Edit Strength (DS $\uparrow$**)** DS measures how much has the steered image moved towards the target concept c_A in CLIP space t_A: $\cos(z'_{\text{CLIP}}, t_A) - \cos(z_{\text{CLIP}}, t_A)$. A positive value indicates successful semantic steering towards the target, and a value near zero means no meaningful edit.

2. Protected Concept Drift ($D_p \downarrow$**)** D_p quantifies how much non-target attributes in the protected set $\mathcal{P}$ changed: $\frac{1}{|\mathcal{P}|}\sum_{t_i \in \mathcal{P}} \left|\cos(\text{CLIP}(x'_0), t_i) - \cos(\text{CLIP}(x_0), t_i)\right|$. A low value means non-target attributes were preserved during steering, and that the target concept was successfully disentangled from the protected concepts.

3. Learned Perceptual Image Patch Similarity (LPIPS $\downarrow$). LPIPS (Zhang et al., 2018) measures perceptual deviation between the steered and original image by comparing unit-normalized deep features from a pretrained AlexNet (Krizhevsky et al., 2012). Lower values indicate better perceptual preservation, while higher values reflect larger semantic and structural changes.

Three methods are compared in this paper. Firstly, the **unconstrained** method is the baseline, where the anchor and protected concept drift terms are set to zero. This is a common approach in literature for steering towards a target concept (Zou et al., 2023; Beaglehole et al., 2026). Secondly, the **anchor-only** method with protected concept drift set to zero. This is an ablation to determine if the protected concept term helps in preserving the non-target concepts in the base image. Finally, the proposed **constrained** method is with with all loss terms active.

Experimental Settings. As shown in Table 1, nine concepts are tested. 8 prompts for each concept in the contrastive pair (c_A, c_B) are in Appendix A.2. We set the steering weight $\lambda_t = 5$, protection weight $\lambda_p = 2$ and anchor weight $\lambda_a = 2$, with the intuition of giving more weightage to steering than the other two. Two α values are calculated with the cosine distance between t_A and $t_B \in 0.85, 0.95$, and the average quantitative results are reported. Additional details on experimental setup are in Appendix in Table 3.

4.1. Quantitative Results

Table 2 shows the results averaged over the nine concepts, and Table 1 shows the results across all nine concepts.

Overall, the DS metric, which shows raw target motion, favors the unconstrained baseline on average: unconstrained has the highest mean DS and achieves the best results on 2 out of 9 concepts. That is expected as unconstrained does not trade DS against unwanted changes to other concepts. The constrained method performs best on 4 concepts. The proposed method achieves the best (lowest) D_p in 7 out of 9 pairs. Therefore, the constrained method consistently reduces non-target drift. Likewise, LPIPS is the best on average for the constrained steering. However, per concept, the LPIPS metric results are mixed, with all methods winning on some pairs. This is expected as LPIPS measures overall perceptual change, not semantic correctness or disentanglement.

4.2. Qualitative Results

In Fig. 2, we show steered images for four concept pairs across a range of α values. As α increases, the target concept is applied more strongly while the influence of protected concepts and the anchor diminishes, allowing greater deviation from the original image. Moderate α values best preserve identity and secondary attributes, whereas extreme values can introduce drift.

Young vs. Old. Age shifts are subtle but discernible: positive α produces younger, baby-like faces, while negative α yields more aged appearances. At large $|\alpha|$, species drift begins to emerge.

Light vs. Dark. Coat color shifts from dark to light as α increases, while expression and fur texture remain largely preserved at moderate α.

Dog vs. Cat. Across diverse starting images, increasing α drives a clear species transition from dog-like to intermediate fox- or wild-like faces to cat-like appearances, while fur color and texture are mostly maintained.

Table 1. Individual results on steering of 9 target concepts (c_A). Best value per metric is in **bold**.

CONTRASTIVE PAIR	UNCONSTRAINED			**Constrained (ours)**			Anchor-only		
c_A / c_B	DS↑	D_p↓	LPIPS↓	DS↑	D_p↓	LPIPS↓	DS↑	D_p↓	LPIPS↓
Striped / Plain	.0114	**.0118**	**.233**	**.0138**	.0182	.287	.0104	.0167	.303
Cat / Dog	.0465	.0295	.375	.0400	**.0223**	**.342**	**.0480**	.0275	.367
Wild / Domestic	.0066	.0153	**.194**	**.0101**	**.0125**	.231	.0071	.0127	.195
Young / Old	.0029	.0127	.185	.0019	**.0114**	.184	**.0042**	.0120	**.159**
Light / Dark	**.0166**	.0230	.261	.0144	**.0229**	**.252**	.0042	.0311	.278
Aggr. / Gentle	**.0050**	.0131	.181	.0040	**.0130**	**.153**	.0032	.0153	.186
Fluffy / Sleek	.0063	.0144	.239	−.0005	**.0118**	**.157**	**.0078**	.0119	.184
Pointed / Floppy ears	.0097	**.0124**	.226	**.0145**	.0175	.199	.0100	**.0124**	**.177**
Green / Brown eyes	.0113	.0192	**.208**	**.0120**	**.0130**	.211	.0119	.0184	.243

Figure 2. Steering results across four concept pairs: young/old (top left), dog/cat (top right), dark/light (bottom left), and gentle/aggressive (bottom right). Small α preserves non-target attributes, while larger α produces stronger, less constrained edits.

Gentle vs. Aggressive. Expressions shift continuously from peaceful to fierce as α increases, with species identity well-preserved at middling α values.

5. Concluding remarks

We introduce a framework for interpreting and steering diffusion models by aligning Koopman-distilled latents with CLIP's semantic space and finding disentangled edit directions through optimization. The method enables disentangled semantic manipulation while treating the generator as a black box. Quantitative and qualitative results across nine concept pairs demonstrate reduced non-target drift, improved perceptual stability, and smooth transitions along semantic axes. The results highlight how CLIP alignment transforms Koopman latents into a usable semantic interface, enabling targeted edits while keeping the diffusion generator fully frozen.

Table 2. Aggregate Results averaged over 9 Target Concepts.

Method	DS ↑	D_p ↓	LPIPS ↓
Unconstrained	**0.0129**	0.0168	0.2334
Constrained (ours)	0.0122	**0.0159**	**0.2239**
Anchor-only	0.0119	0.0176	0.2324

Acknowledgments

This material is based on work supported by the United States Air Force and Defense Advanced Research Projects Agency (DARPA) under Contract No. FA8750-23-C-0519 and under Agreement No. HR0011-24-9-0424. The views, opinions and/or findings expressed are those of the author and should not be interpreted as representing the official views or policies of the Department of War or the U.S. Government.

Impact Statement

This work advances the interpretability of diffusion models by introducing a principled framework that aligns Koopman-distilled latent representations with CLIP's semantic space, enabling controllable and disentangled image editing without modifying the underlying generator. By formulating semantic steering as a constrained optimization problem, the method explicitly balances target concept manipulation with preservation of non-target attributes, reducing unintended drift and improving perceptual stability compared to existing approaches. The proposed black-box strategy lowers the barrier to analyzing and controlling complex generative models, offering a scalable and model-agnostic interface for semantic manipulation. This has broad implications for safer and more transparent deployment of generative AI systems, particularly in applications requiring fine-grained control and reliability, while also contributing to the growing effort toward interpretable and steerable foundation models.

References

Anthropic. Claude opus 4.6, 2026. URL https://www.anthropic.com. Large language model. Accessed 2026-05-08.

Bai, H., Ding, W., and Zou, D. Hierarchical koopman diffusion: Fast generation with interpretable diffusion trajectory. *Advances in Neural Information Processing Systems*, 38:87345–87379, 2026.

Beaglehole, D., Radhakrishnan, A., Boix-Adsera, E., and Belkin, M. Toward universal steering and monitoring of ai models. *Science*, 391(6787):787–792, 2026.

Becker, J., Wendler, C., Baylies, P., West, R., and Wressnegger, C. Controlling latent diffusion using latent clip. *arXiv preprint arXiv:2503.08455*, 2025.

Berman, N., Naiman, I., Eliasof, M., Zisling, H., and Azencot, O. One-step offline distillation of diffusion-based models via koopman modeling. *Advances in Neural Information Processing Systems*, 38:14776–14811, 2026.

Epstein, D., Jabri, A., Poole, B., Efros, A., and Holynski, A. Diffusion self-guidance for controllable image generation. *Advances in Neural Information Processing Systems*, 36:16222–16239, 2023.

Hertz, A., Mokady, R., Tenenbaum, J., Aberman, K., Pritch, Y., and Cohen-Or, D. Prompt-to-prompt image editing with cross attention control. *arXiv preprint arXiv:2208.01626*, 2022.

Huang, Y., Huang, J., Liu, Y., Yan, M., Lv, J., Liu, J., Xiong, W., Zhang, H., Cao, L., and Chen, S. Diffusion model-based image editing: A survey. *IEEE Transactions on Pattern Analysis and Machine Intelligence*, 2025.

Koopman, B. O. Hamiltonian systems and transformation in hilbert space. *Proceedings of the National Academy of Sciences*, 17(5):315–318, 1931.

Krizhevsky, A., Sutskever, I., and Hinton, G. E. Imagenet classification with deep convolutional neural networks. *Advances in neural information processing systems*, 25, 2012.

Park, Y.-H., Kwon, M., Choi, J., Jo, J., and Uh, Y. Understanding the latent space of diffusion models through the lens of riemannian geometry. *Advances in Neural Information Processing Systems*, 36:24129–24142, 2023.

Radford, A., Kim, J. W., Hallacy, C., Ramesh, A., Goh, G., Agarwal, S., Sastry, G., Askell, A., Mishkin, P., Clark, J., et al. Learning transferable visual models from natural language supervision. In *International conference on machine learning*, pp. 8748–8763. PmLR, 2021.

Tinaz, B., Fabian, Z., and Soltanolkotabi, M. Emergence and evolution of interpretable concepts in diffusion models. *Advances in neural information processing systems*, 38:166943–166986, 2026.

Zhang, R., Isola, P., Efros, A. A., Shechtman, E., and Wang, O. The unreasonable effectiveness of deep features as a perceptual metric. In *Proceedings of the IEEE conference on computer vision and pattern recognition*, pp. 586–595, 2018.

Zou, A., Phan, L., Chen, S., Campbell, J., Guo, P., Ren, R., Pan, A., Yin, X., Mazeika, M., Dombrowski, A.-K., et al. Representation engineering: A top-down approach to ai transparency. *arXiv preprint arXiv:2310.01405*, 2023.

A. Appendix

A.1. Vocabulary scoring prompts

Prompts can be selected from a broader candidate set derived from attributes of open-source dataset, filtered for the target categories and cleaned to remove noisy or ambiguous descriptions. These prompts are then scored against a held-out set of validation images via cosine similarity between the CLIP embeddings of the image and the prompt. Candidates are grouped into categories by first clustering the validation images in CLIP embedding space into K_{img} groups. Then, each prompt is scored over each image cluster, which for a prompt t_i over image cluster c is

$$s(t_i, c) = \frac{1}{|c|} \sum_{x \in c} \cos(\mathrm{CLIP}_{\mathrm{img}}(x),\, \mathrm{CLIP}_{\mathrm{txt}}(t_i)) \tag{4}$$

These scores are concatenated to give a vector of length K_{img} per prompt, describing how strongly that prompt activates across different image categories. The prompt's own CLIP text embedding is appended to this vector, and a second k-means pass is run. This yields a set of prompt categories that classify prompts that are both semantically similar and activate on similar images. A balanced selection retains the highest-scoring prompts per category subject to minimum mean-score and diversity thresholds.

A.2. Prompts for Contrastive Pairs of Each concept

Prompts for constrastive pairs of all 9 concepts are generated with Opus 4.6 (Anthropic, 2026): for each concept c_A (or c_B), all strings below are CLIP-encoded, and averaged. The difference between the average encoded contrastive concepts $(t_A - t_B)$ is used to define the target direction.

Five pairs use the same template with concept phrases c as shown below and the remaining four used different prompts for different pairs.

Template (8 prompts per concept) . For concept phrase c, the prompts are: `a photo of` c; `an animal face that is` c; `a realistic animal photo showing` c; `a high quality photo of` c; `a centered portrait of` c; c`, wildlife photography`; `a detailed image of` c; c `looking at the camera`.

`striped_vs_plain` (template). **concept A** ($c_A =$ `a striped animal`): apply the ten-template list above with this c_A.
concept B ($c_B =$ `a plain solid-colored animal`): same with c_B.

`wild_vs_domestic` (template). **concept A** ($c_A =$ `a wild ferocious animal`).
concept B ($c_B =$ `a calm domestic pet`).

`light_vs_dark` (template). **concept A** ($c_A =$ `a light white animal`).
concept B ($c_B =$ `a dark black animal`).

`pointed_ears_vs_floppy` (template). **concept A** ($c_A =$ `an animal with pointed erect ears`).
concept B ($c_B =$ `an animal with floppy droopy ears`).

`green_eyes_vs_brown` (template). **concept A** ($c_A =$ `an animal with bright green eyes`).
concept B ($c_B =$ `an animal with dark brown eyes`).

`species_cat_vs_dog` (custom). **concept A:**

- `a close-up cat face`
- `a domestic cat face`
- `a tabby cat portrait`
- `a feline animal face`

- a house cat looking at the camera
- a realistic photo of a cat face
- a centered portrait of a cat
- a cat with pointed ears and whiskers

concept B:

- a close-up dog face
- a domestic dog face
- a puppy or dog portrait
- a canine animal face
- a pet dog looking at the camera
- a realistic photo of a dog face
- a centered portrait of a dog
- a dog with a snout and floppy ears

`young_vs_old` (custom). concept A:

- a young puppy face
- a baby animal face
- a juvenile animal face
- a small young pet face
- a young animal with soft features
- a cute young animal face
- a youthful animal portrait
- a young animal with bright eyes

concept B:

- an old animal face
- an elderly dog face
- an aged animal with gray fur
- a senior pet face
- an old animal with tired eyes
- an elderly animal portrait
- an animal with old facial features
- a mature old animal face

`aggressive_vs_gentle` (custom). concept A:

- an aggressive angry animal
- an animal with intense angry eyes
- a fierce animal face
- a threatening animal expression

- `an animal looking aggressive`
- `a hostile animal face`
- `an animal with a fierce stare`
- `an angry animal portrait`

concept B:

- `a gentle peaceful animal`
- `a calm friendly animal face`
- `a relaxed animal expression`
- `a peaceful pet face`
- `an animal with soft gentle eyes`
- `a friendly animal portrait`
- `a calm animal looking at the camera`
- `a non-threatening animal face`

`fluffy_vs_sleek` (custom). **concept A:**

- `a fluffy furry animal`
- `an animal with thick fluffy fur`
- `a long-haired animal face`
- `a soft fluffy pet`
- `a furry animal with dense coat`
- `a shaggy animal face`
- `an animal with soft thick fur`
- `a fluffy animal portrait`

concept B:

- `a sleek short-haired animal`
- `an animal with short smooth fur`
- `a short-haired pet face`
- `a smooth-coated animal`
- `an animal with sleek fur`
- `a clean short coat animal`
- `an animal with no fluffy fur`
- `a sleek animal portrait`

A.3. Experimental Setup

Table 3 shows detailed experimental setup.

Table 3. Experimental setup.

Item	**Value**
Generative model	Frozen KDM (EMA checkpoint), 50K generated 64×64 images
Generated Images	Test: 40k, Val: 10k
CLIP bridge	$\mathrm{Enc}_{\mathrm{clip}}$ / $\mathrm{Dec}_{\mathrm{clip}}$ (ViT-B/32)
Concept vocabulary	Visual Genome–derived, AFHQ-filtered (96 prompts)
Concept pairs	9 contrastive pairs (Table 1)
α values	Reported results are average over two target cosine distance between $t_A, t_B \in \{0.95, 0.85\}$
Constrained optimization	
Loss weights	$\lambda_{\mathrm{target}}=5,\ \lambda_{\mathrm{protect}}=2,\ \lambda_{\mathrm{anchor}}=2$
Optimizer	Adam, lr=0.02, 30 steps

Direction	Base Image	Protected Concepts (Vocabulary)	Final Image
Cat		• `a photo of a tiger gray` (0.307) • `a stripe white animal` (0.292) • `a white orange animal` (0.273) • `a colored white animal` (0.270) • `an animal with black white face` (0.264) • `an animal with gray collar` (0.262) • `a outdoor light animal` (0.261) • `an animal with face head` (0.261)	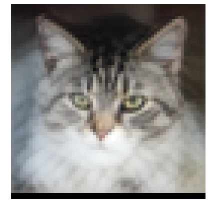
Light	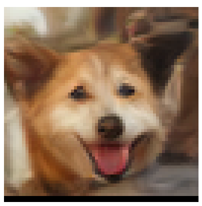	• `a photo of a tired dog` (0.257) • `an animal with red fur` (0.249) • `a photo of a fox` (0.248) • `a fluffy animal` (0.246) • `an animal with yellow hair` (0.240) • `an animal with red eye` (0.239) • `an animal with head` (0.235) • `an animal with long curly hair` (0.229)	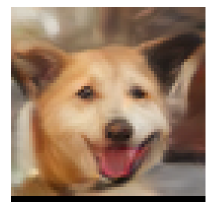
Old	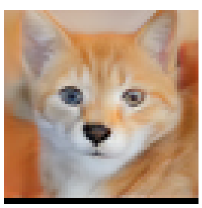	• `a photo of a cat orange` (0.292) • `a white orange animal` (0.273) • `a orange striped animal` (0.266) • `a photo of a fox` (0.251) • `a light blonde animal` (0.248) • `a light colored animal` (0.245) • `an animal with white fur` (0.245) • `an animal with green eye` (0.243)	
Aggressive	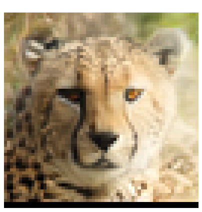	• `a spotted pattern animal` (0.284) • `a outdoor light animal` (0.277) • `an animal with white face` (0.277) • `a black spotted animal` (0.276) • `a red spot animal` (0.272) • `an animal with face head` (0.271) • `an animal with green eye` (0.269) • `a photo of a tiger gray` (0.268)	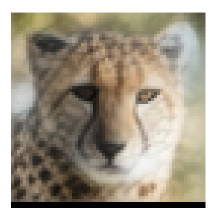

Table 4. Examples of selected protected concepts across different steering directions at inference time for the base image. For each base image, the optimizer holds the listed visual attributes constant while pushing the latent in the target direction. The values in parentheses denote the initial CLIP cosine similarity scores between the base image and the text prompt, which are used to select the top concepts.